Impedance Differential Protection for Double Circuit transmission Lines Based on Distributed Parameters

Talib M. Challab, H. Seyedi* and N. Rostami

Faculty of Electrical and Computer Engineering, University of Tabriz, Tabriz, Iran

Abstract- *This paper presents an impedance differential protection scheme for a double circuit transmission line. Current and voltage measurements at both line ends enable the formulation of a differential impedance that serves as an effective protection standard for transmission lines. The proposed method takes into consideration the effects of the line's shunt capacitance since it is based on the distributed parameter line model. The proposed protection system is able to detect the faults and also has the ability to determine the fault location. In addition, the relay offers dependability, and selectivity for differentiating between internal and external faults, thereby stays steady against external faults. The proposed method has been tested with varying fault resistances and under various fault conditions. The effectiveness, security, and dependability of the method are verified by the simulation results.*

Keywords*: Impedance differential protection, double-circuit line, transmission line, distributed parameters.*

I. INTRODUCTION

In today's power networks, double-circuit transmission lines play an essential role [1]. Double-circuit transmission lines are widely used in modern power systems to improve the reliability and security of electrical energy transmission. They are frequently hundreds of kilometers long and serve as essential interconnections between energy production and consumption hubs. The mutual coupling effect, together with the various topologies of double-circuit lines, results in a wide number of probable fault types on double-circuit lines. Therefore, protection of double circuit lines and estimation of fault location are regularly challenging tasks [2]. Techniques for detecting, classifying, and locating faults in power systems have advanced rapidly over the last two decades. Communication systems, signal processing techniques, global positioning systems (GPS), artificial intelligence systems, and machine learning have all advanced, allowing more in-depth studies into fault protection approaches to be conducted. Due to technological and procedural limitations in identifying and finding defects in real-time monitoring, the locations of faults were previously difficult to ascertain. The precision and dependability of the suggested method were important factors in determining the location of a defect [3]. Thus far, various protection schemes for the double-circuit line have been proposed. [4] presents one form of protection based on the dynamic state estimation method. Another approach to double circuit transmission line protection based on system impedance, varying power swing slip frequency, and infeed effect is presented in [5]. Double circuit transmission line protection based on the current differential method is one of the oldest methods of protection and continues to be used and even, in the case of short lines, dominates other protection schemes, since it is considered superior with respect to selectivity, sensitivity, stability and speed of operation as compared with other forms of protection. In [6] , a current differential protection method has been presented based on modal transformation matrix and using the sum of ratios of modal currents given in [7]. In [8] the differential protection methodology based on superimposed component of current, while [9] proposes transverse differential protection based on impedance comparison of the parallel circuits measured at one end. However, cross protection alone cannot operate if one of the transmission line is out of service. In [10] a new backup protection scheme has been proposed by computing and comparing the absolute difference of superimposed voltages (ADSV) at the tap-point (T-point). A differential relaying technique based on the DWT (Discrete Wavelet Transform) approach is employed to identify and categorize transmission line fault patterns in [11]. [12] presents one form of protection based on cutting-edge Cos-Sin features. In [13] another method of the protection scheme for double-circuit transmission lines uses a Convolutional Neural Network (CNN). Interestingly, [14] presents novel fuzzy distance protection, while Ref. [15] mentioned that, most of the presented parallel transmission line protection can be categorized into non-communication impedance techniques. The authors of [16] propose a new fault-loop impedance measurement algorithm for inter-circuit faults on double-circuit lines. In [17] a new standby relay protection scheme based on overcurrent and directional elements is proposed. But the application of the method is limited to radial power flow networks with pre-fault current direction known. [18] also presents a protection scheme for double circuit transmission line based on traveling wave protection. Another form of protection method based on the Wavelet transform technique is presented by [19]. The protective relaying functions of the SCCDCTL is proposed [20] based on DWT and K-nearest neighbor (KNN) algorithm. [21] has described other methods of protection schemes based on Artificial Neural Networks (ANN). Artificial-neural-network based approach is used for fault detection, fault phase selection and fault classification in [22] as well. The longitudinal current differential protection algorithm is commonly used for parallel lines installed on one tower [23]. However, such a protective relay depends on a communication route and is affected by dispersed capacitance [24]. The distance protection intended for parallel lines presented in [25] faces some problems, mostly due to mutual coupling between the circuits. It causes the relay become overreached or under-reached depending on the network parameters, operating state, and location of the fault [26]. To improve the relay performance an application of adaptive protection techniques is proposed in [27]. Other available protection options for double-circuit lines are related current transverse differential protection including directional transverse differential protection [28]. Their operation is not dependent on channels of communication but exit a long successive operating zone. This study provides a negative sequence current-based scheme for finding faults and identifying problematic circuit lines. However, it has the shortcoming of not being able to compute the fault location in balanced three-phase failures [29].

This article deals with the impedance-differential protection methods providing effective protection of transmission lines [30]. The traditional current differential relays use measurements of three-phase currents at the line ends, while the impedance-differential protection method, first introduced in [30] applies the measurements of both currents and voltages from the line ends. Thus, more information on the fault is provided. Based on the voltage and current measurements from both line ends, the differential impedance is calculated. This method is able to detect reliably internal faults regardless of the transmission line length. In addition, the impedance-differential protection method provides the fault location with high accuracy. This method was precisely described in [30] and improved in [31]. However, the original impedance-differential protection scheme is based on the lumped parameters model of the transmission lines. Therefore, in the case of long transmission lines, the accuracy of original method is affected by the capacitive charging currents. In this paper, it has been tried to enhance the accuracy of impedance-differential protection method by applying the distributed parameter line model. Furthermore, the new method takes into account the mutual coupling effect of double circuit transmission line, while the original method has only been applied to the single circuit lines.

II. IMPEDANCE DIFFERENTIAL PROTECTION FOR DOUBLE-CIRCUIT TRANSMISSION LINE

The equivalent double circuit line model shown in Fig. 1 is used for the analysis of transmission line fault during symmetrical and asymmetrical faults. The effect of mutual coupling should be considered for incisive analysis of double circuit lines, since the dominant zero sequence mutual impedance has the main role to play in asymmetrical fault case.

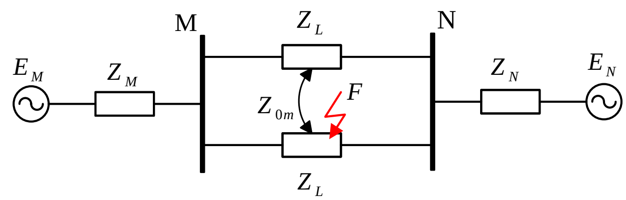

Fig. 1 The schematic diagram of the double-circuit line.

For this purpose, in this study, the analysis of the symmetrical components is utilized. Here, the subscripts 1, 2, and 0 denote the positive, negative, and zero sequence components, respectively. Fig. 2 represents the positive, negative, and zero sequence network for a double-circuit line. Using Fig. 2, the positive, negative and zero sequence voltages of the fault point are calculated from both M and N terminals. Then, the corresponding values are set equal to each other. The results are presented in (1):

$$\begin{aligned}
&\bar{U}_{f1} = \bar{U}_{m1}\cosh(\gamma_1 d) - z_{c1}(\bar{I}_{m1})\sinh(\gamma_1 d) = \\
&\bar{U}_{n1}\cosh(\gamma_1(D-d)) - z_{c1}(\bar{I}_{n1})\sinh(\gamma_1(D-d)) \\
&\bar{U}_{f2} = \bar{U}_{m2}\cosh(\gamma_1 d) - z_{c1}(\bar{I}_{m2})\sinh(\gamma_1 d) = \\
&\bar{U}_{n2}\cosh(\gamma_1(D-d)) - z_{c1}(\bar{I}_{n2})\sinh(\gamma_1(D-d)) \\
&\bar{U}_{f0} = \bar{U}_{m0}\cosh(\gamma_0 d) - z_{c0}(\bar{I}_{m0})\sinh(\gamma_0 d) - z_{0m} d\,(\bar{I}^h_{m0}) = \\
&\bar{U}_{n0}\cosh(\gamma_0(D-d)) - z_{c0}(\bar{I}_{n0})\sinh(\gamma_0(D-d)) - z_{0m}(D-d)(\bar{I}^h_{n0})
\end{aligned} \tag{1}$$

where:

$\bar{U}_{m1}, \bar{U}_{m2}, \bar{U}_{m0}$– symmetrical components of voltage from the joint bus M,

$\bar{U}_{n1}, \bar{U}_{n2}, \bar{U}_{n0}$– symmetrical components of voltage from the joint bus N,

$\bar{I}_{m1}, \bar{I}_{m2}, \bar{I}_{m0}$– symmetrical components of current at bus M,

$\bar{I}_{n1}, \bar{I}_{n2}, \bar{I}_{n0}$ – symmetrical components of current at bus N,

D – length of the line (km),

d – unknown distance, counted from bus M to fault F

$\gamma_1 = \sqrt{Z_1 Y_1}$– propagation constant of the line for the positive-sequence (negative-sequence),

$\gamma_0 = \sqrt{Z_0 Y_0}$– propagation constant of the line for the zero-sequence,

$Z_{c1} = \sqrt{Z_1/Y_1}$ – characteristic impedance of the line for the positive-sequence (negative-sequence),

$Z_{c0} = \sqrt{Z_0/Y_0}$ – characteristic impedance of the line for the zero-sequence,

$Z_1 = R_1 + j\omega_1 L_1$ – impedance of the line for the positive-sequence (negative-sequence) (Ω/km),

$Z_0 = R_0 + j\omega_1 L_0$ – impedance of the line for the zero-sequence (Ω/km),

$Y_1 = G_1 + j\omega_1 C_1$ – admittance of the line for the positive-sequence (negative-sequence) (S/km),

$Y_0 = G_0 + j\omega_1 C_0$ – admittance of the line for the zero-sequence (S/km),

R_1, L_1, G_1, C_1 – resistance, inductance, conductance and capacitance of the line for the positive-sequence (negative-sequence) per km length,

R_0, L_0, G_0, C_0 – resistance, inductance, conductance and capacitance of the line for the zero-sequence per km length,

$\bar{I}^h_{m0}, \bar{I}^h_{n0}$ – zero-sequence currents of the healthy line at the terminals M and N, respectively.

Z_{0m} – zero sequence mutual coupling line impedance.

Assuming that phase-a is exposed to the fault, and after implementation of symmetrical component properties, which can be obtained from (1). The equation (2) can be defined as

$$\begin{aligned}
&\bar{U}_{ma}\cosh(\gamma_1 d) - \bar{U}_{na}\cosh(\gamma_1(D-d)) - \\
&z_{c0}\sinh(\gamma_0 d)(\bar{I}_{m0}) + z_{c1}\sinh(\gamma_1 d)(\bar{I}_{m0}) + \\
&z_{c0}\sinh(\gamma_0(D-d))(\bar{I}_{n0}) - z_{c1}\sinh(\gamma_1(D-d))(\bar{I}_{n0}) - \\
&z_{0m} d\,(\bar{I}^h_{m0}) + z_{0m}(D-d)(\bar{I}^h_{n0}) = \\
&z_{ca}(\bar{I}_{m1})\sinh(\gamma_1 d) - z_{c1}(\bar{I}_{na})\sinh(\gamma_1(D-d))
\end{aligned} \tag{2}$$

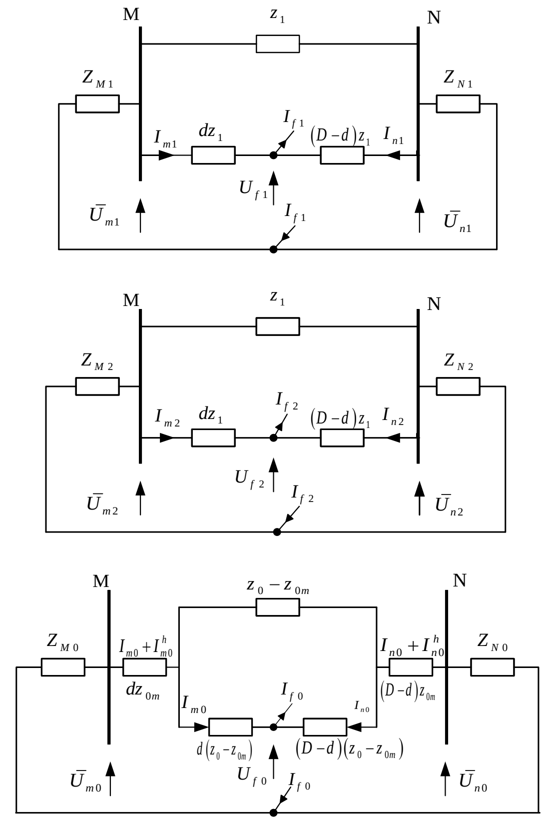

Fig. 2 Equivalent circuit diagram of double-circuit line for: positive, negative and zero-sequence components

In view of zero-sequence circuit presented in Fig. 2, the equation (2) can be defined as:

$$\begin{aligned}
&\bar{U}_{ma}\cosh(\gamma_1 d) - \bar{U}_{na}\cosh(\gamma_1(D-d)) - \bar{U}_{m0}\cosh(\gamma_0 d) + \\
&\bar{U}_{n0}\cosh(\gamma_0(D-d)) + z_{c1}\sinh(\gamma_1 d)(\bar{I}_{m0}) - z_{c1}\sinh(\gamma_1(D-d))(\bar{I}_{n0}) = \\
&z_{c1}(\bar{I}_{ma})\sinh(\gamma_1 d) - z_{c1}(\bar{I}_{na})\sinh(\gamma_1(D-d))
\end{aligned} \tag{3}$$

The unknown variables d_1, d_2 for symmetrical and asymmetrical faults, can be derived from positive-sequence and zero-sequence components analysis respectively, and can be expressed as:

$$d_1 = \frac{\begin{aligned}&\bar{U}_{n1}\left(\cosh(\gamma_1(D-d_0)) + d_0\gamma_1\sinh(\gamma_1(D-d_0))\right) - \\ &z_{c1}(\bar{I}_{n1})\left(\sinh(\gamma_1(D-d_0)) + d_0\gamma_1\cosh(\gamma_1(D-d_0))\right) - \\ &\bar{U}_{m1}\left(\cosh(\gamma_1 d_0) - d_0\gamma_1\sinh(\gamma_1 d_0)\right) + \\ &z_{c1}(\bar{I}_{m1})\left(\sinh(\gamma_1 d_0) - d_0\gamma_1\cosh(\gamma_1 d_0)\right)\end{aligned}}{\begin{aligned}&\bar{U}_{m1}\gamma_1\sinh(\gamma_1 d_0) - z_{c1}(\bar{I}_{m1})\gamma_1\cosh(\gamma_1 d_0) + \\ &\bar{U}_{n1}\gamma_1\sinh(\gamma_1(D-d_0)) - z_{c1}(\bar{I}_{n1})\gamma_1\cosh(\gamma_1(D-d_0))\end{aligned}} \tag{4}$$

$$d_2 = \frac{\begin{array}{l}\bar{U}_{n0}\left(\cosh\left(\gamma_0\left(D-d_0\right)\right)+d_0\gamma_0\sinh\left(\gamma_0\left(D-d_0\right)\right)\right)- \\ z_{c0}\left(\bar{I}_{n0}\right)\left(\sinh\left(\gamma_0\left(D-d_0\right)\right)+d_0\gamma_0\cosh\left(\gamma_0\left(D-d_0\right)\right)\right)- \\ \bar{U}_{m0}\left(\cosh\left(\gamma_0 d_0\right)-d_0\gamma_0\sinh\left(\gamma_0 d_0\right)\right)+ \\ z_{c0}\left(\bar{I}_{m0}\right)\left(\sinh\left(\gamma_0 d_0\right)-d_0\gamma_0\cosh\left(\gamma_0 d_0\right)\right)-z_{0m}D\left(\bar{I}^h_{n0}\right)\end{array}}{\begin{array}{l}\bar{U}_{m0}\gamma_0\sinh\left(\gamma_0 d_0\right)-z_{c0}\left(\bar{I}_{m0}\right)\gamma_0\cosh\left(\gamma_0 d_0\right)+ \\ \bar{U}_{n0}\gamma_0\sinh\left(\gamma_0\left(D-d_0\right)\right)-z_{c0}\left(\bar{I}_{n0}\right)\gamma_0\cosh\left(\gamma_0\left(D-d_0\right)\right)- \\ z_{0m}\left(\bar{I}^h_{m0}+\bar{I}^h_{n0}\right)\end{array}} \quad (5)$$

From Equations (3), (4), and (5), the impedance difference Z'diff can be defined in single phase faults as:

$$Z'_{diff} = \frac{\begin{array}{l}\bar{U}_{ma}\cosh\left(\gamma_1 d\right)-\bar{U}_{na}\cosh\left(\gamma_1\left(D-d\right)\right)- \\ \bar{U}_{m0}\cosh\left(\gamma_0 d\right)+\bar{U}_{n0}\cosh\left(\gamma_0\left(D-d\right)\right)+ \\ z_{c1}\sinh\left(\gamma_1 d\right)\left(\bar{I}_{m0}\right)-z_{c1}\sinh\left(\gamma_1\left(D-d\right)\right)\left(\bar{I}_{n0}\right)\end{array}}{\bar{I}_{ma}-\bar{I}_{na}}$$

(6)

In the first stage, information related to each phase (ϕ) voltages and currents from both line ends is gathered and the fault detection criterion is checked. This step allows to discriminate normal and faulty conditions in the protected line. The criterion is expressed as:

$$\left|\bar{I}_{m\phi}\right|+\left|\bar{I}_{n\phi}\right| > I_{com} \quad (7)$$

Where I_{com} is a threshold value. If the fault condition is fulfilled, in the next step, the compensated differential impedance in (6) is computed. It is assumed that the fault (F) is on the line M-N, at the relative distance FD, counted from the bus M, being calculated by the proposed method and it is more accurate than d (d_1, d_2), which also represents the location of the fault, which was calculated with positive and zero sequence components. Thereafter, the fault location can be determined using:

$$FD = \frac{1}{2}\times\left(\frac{\mathrm{Im}\left(Z_{Lp}\right)}{\mathrm{Im}\left(zD\right)}+1\right)\times D \quad (8)$$

where Z_{Lp} is calculated from:

$$Z_{Lp} = \left(Z'_{diff}-\frac{zD}{2}\right)\times\frac{I_{ma}-I_{na}}{I_{ma}+I_{na}} \quad (9)$$

The algorithm checks whether the fault is internal or external based on (10), where D_{com} is set to 0.05D in this study.

$$\left|FD-0.5D\right| > D_{com} \quad (10)$$

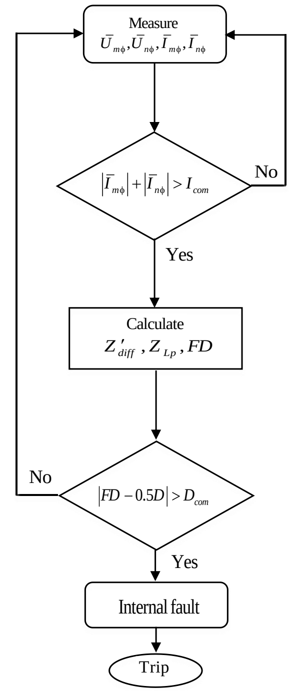

Fig. 3 Flowchart of the proposed protection scheme

III. SIMULATION RESULTS

For evaluating the presented algorithm, it has been tested on a 500 kV, 50 Hz, two-machine system, as shown in Figure 3 1. The system data are given in Table 1 and Table 2. Moreover, the simulation is performed in MATLAB SIMULINK. The sampling frequency is 2 kHz and phasor estimation is performed by the full cycle Fourier filtering. In order to test the proposed protection algorithm, short-circuit simulations have been conducted inside the line. Different line lengths 80 km, 240 km, and 400 km have been taken under consideration whereas the faults have been applied inside the protected zone. Moreover, P1, P2, P3, P4, and P5 are located inside the protected line at d=0, d=D/4, d=D/2, d=3D/4, and d=D, respectively, where D is the total length of the protected line. The studies included four different short-circuit types: three-phase fault (ABCG) and different types of asymmetrical faults, phase-to-earth (AG), phase-to-phase (AB), and phase-to-phase-to-earth (BCG) faults. By analyzing the results obtained for all types of faults, it was found that they are more accurate compared to the results in [30], where the average accuracy of the results reaches 99.870, while the average results in [30] were 99.803, according to the results presented and for all types of faults as well.

Table 1*: Impedance Sources in The Simulated System*

System element	Parameter	
Equivalent system-N	Z_{N1}	(2.615+ j14.829)Ω
	Z_{N2}	(4.637 + j26.297)Ω
	Voltage phase angle	0^0
Equivalent system-M	Z_{M1}	$= 2Z_{N1}$
	Z_{M2}	$= 2Z_{N0}$
	Voltage phase angle	-30^0

Table 2*: Transmission Line Impedance Parameters*

System element	Parameter	
Transmission line	Z_1	(0.0276 + j0.315) Ω/km
	Z_0	(0.275 + j1.0265) Ω/km
	Z_{0m}	(0.21 + j0.628) Ω/km
	C_1	13 nF/km
	C_0	8.5 nF/km
	C_{0m}	5 nF/km

A. Effects of Line Length

These effects have been investigated using three different lengths encompassing short, medium, and long transmission lines. In order to evaluate the effect of the length of lines on the impedance differential protection. Table 3 and Table 4 show the simulation results obtained by applying the proposed method to different fault types at different locations. As shown in Tables 3, 4 the proposed scheme has a reliable performance regardless of line length. In addition to the tabular results, the dynamic performance of the proposed scheme is shown for some operational conditions in Fig. 4 to Fig. 6. For example, Fig. 4 and Fig. 5 show the voltage and current of three-phase in the case of AB fault at 200km, respectively. Fig. 6 represents the FD for a three-phase fault at 200 km of line MN at the instant of 0.1s. After 0.2s from the fault inception, the calculated FD is close to the steady-state value of 200 km.

In the following tables, the percentage error of computed fault location is defined as

$$Error\,(\%) = \frac{|\text{Computed location - Actual location}|}{\text{Line length}} \times 100 \qquad (11)$$

Table 3*: Effects of Line Length at symmetrical faults*

Length Line	Fault Location	Fault Type	Actual Location (km)	Computed Location (FD) (km)	Error (%)
400 (km)	0D	ABCG	0	0.04	0.009
	0.25D	ABCG	100	101.83	0.459
	0.50D	ABCG	200	200.15	0.037
	0.75D	ABCG	300	298.91	0.272
	D	ABCG	400	399.32	0.170
240 (km)	0D	ABCG	0	0.63	0.263
	0.25D	ABCG	60	60.53	0.219
	0.50D	ABCG	120	120.03	0.012
	0.75D	ABCG	180	179.93	0.028
	D	ABCG	240	239.97	0.014
80 (km)	0D	ABCG	0	0.04	0.044
	0.25D	ABCG	20	20.02	0.029
	0.50D	ABCG	40	40.00	0.006
	0.75D	ABCG	60	59.99	0.014
	D	ABCG	80	79.98	0.019

Table 4*: Effects of Line Length at symmetrical faults*

Length Line	Fault Location	Fault Type	Actual Location (km)	Computed Location (FD) (km)	Error (%)
400 (km)	0D	AB	0	1.51	0.378
	0.25D	AB	100	101.51	0.379
	0.50D	AB	200	199.94	0.015
	0.75D	AB	300	298.94	0.264
	D	AB	400	399.39	0.152
240 (km)	0D	BCG	0	0.85	0.356
	0.25D	BCG	60	60.69	0.289
	0.50D	BCG	120	119.97	0.011
	0.75D	BCG	180	180.02	0.007
	D	BCG	240	240.00	0.001
80 (km)	0D	AG	0	0.07	0.091
	0.25D	AG	20	20.04	0.052
	0.50D	AG	40	40.00	0.000
	0.75D	AG	60	59.96	0.046
	D	AG	80	79.95	0.063

B. Effect of The Network Impedance

The proposed method has been tested in the event of network changes. Several short-circuit cases have been simulated by changing the impedance of the equivalent network-the remote side source to 50% and 150% of the actual value. Based on the obtained results shown in Table 5, the performance of the proposed method is proven against topological changes.

Table 5: *B. Effect of The Network Impedance*

Source Impedance	Fault Type	Length Line (km)	Actual Location (km)	Computed Location (km)	Error (%)
50%	ABCG	400	300	298.96	0.259
		240	180	179.89	0.046
		80	60	59.99	0.009
	AB	400	200	200.00	0.000
	BCG	240	120	120.00	0.001
	AG	80	40	40.00	0.001
150%	ABCG	400	300	298.68	0.331
		240	180	179.69	0.129
		80	60	59.99	0.013
	AB	400	200	200.34	0.086
	BCG	240	120	120.01	0.002
	AG	80	40	40.00	0.000

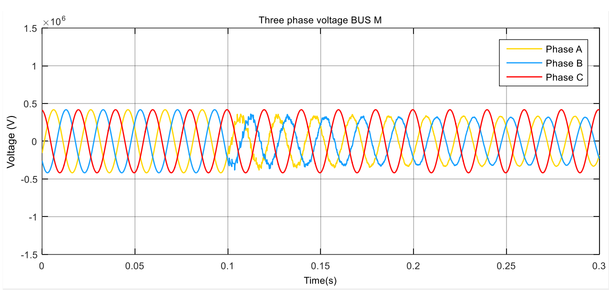

Fig. 4: Three Phase Voltage at Terminal M for an AB Fault

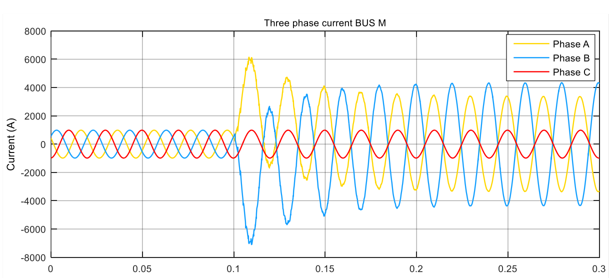

Fig. 5: Three Phase Current at Terminal M for an AB Fault

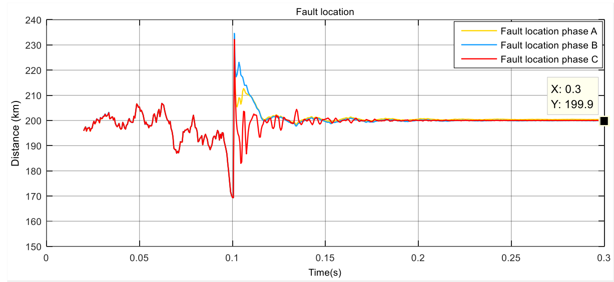

Fig. 6: Computed Fault Location (FD) for an Internal Fault at 200 km

C. Effect of Fault Resistance

In order to check the performance of the proposed method in the resistive earth faults, various faults have been tested with resistance values applied between 0 to 50 Ω. The obtained results are shown in Table 6. it can be concluded that the impedance-based protection algorithm works correctly and is not sensitive to fault resistance. Moreover, the accuracy of the fault location computation remains on the same level and is not influenced by fault resistance.

Table 6*: Effects of Fault Resistance*

Length Line	Fault Type	Actual Location (km)	Fault Resistance (Ω)			Error (%)		
			0	10	50	0	10	50
400 (km)	ABCG	200	199.5	199.5	199.6	0.117	0.114	0.109
	AB	200	200.0	200.3	200.7	0.001	0.067	0.183
	ABCG	300	299.0	298.8	299.3	0.251	0.292	0.172
	AB	300	299.0	299.2	299.6	0.257	0.209	0.095
240 (km)	ABCG	120	120.0	119.9	120.0	0.018	0.022	0.007
	BCG	120	120.0	120.1	120.2	0.008	0.040	0.098
	ABCG	180	179.9	179.9	179.8	0.059	0.050	0.088
	BCG	180	179.8	179.9	180.1	0.072	0.051	0.053
80 (km)	ABCG	40	39.9	39.9	39.9	0.075	0.186	0.067
	AG	40	40.0	39.9	40.3	0.024	0.113	0.363
	ABCG	60	60.1	60.1	60.1	0.123	0.155	0.136
	AG	60	59.9	60.0	60.0	0.098	0.051	0.034

IV. CONCLUSION

In this paper, concepts and features of impedance differential protection for the double-circuit transmission line were introduced. The demonstrated protection algorithm enables not only for internal fault detection, but can be applied also as a fault locator. The method is not affected by the distributed capacitance current because they are based on a distributed parameter line model. Therefore, it does not need to be compensated for the capacitive current in high voltage long transmission lines. The proposed approach works well for double-circuit lines of various lengths and is unaffected by variations in fault resistance. The selectivity is further confirmed because the discussed protection does not function when there are external defects.

V. REFERENCES

[1] M. M. Saha, G. Smetek, J. Izykowski, E. Rosolowski, and P. Pierz, "Location of inter-circuit faults on double-circuit transmission line," Proc. - Int. Conf. Mod. Electr. Power Syst. MEPS 2015, 2015, doi: 10.1109/MEPS.2015.7477199.

[2] G. N. Korres and C. A. Apostolopoulos, "Precise fault location algorithm for double-circuit transmission lines using unsynchronised measurements from two anti-parallel ends," IET Gener. Transm. Distrib., vol. 4, no. 7, pp. 824–835, 2010, doi: 10.1049/iet-gtd.2009.0533.

[3] A. H. Bin Mustapha et al., "Fault location identification of double circuit transmission line using discrete wavelet transform," Indones. J. Electr. Eng. Comput. Sci., vol. 15, no. 3, pp. 1356–1365, 2019, doi: 10.11591/ijeecs.v15.i3.pp1356-1365.

[4] Y. Liu, A. P. Meliopoulos, L. Sun, and R. Fan, "Dynamic state estimation based protection of mutually coupled transmission lines," CSEE J. Power Energy Syst., vol. 2, no. 4, pp. 6–14, 2016, doi: 10.17775/cseejpes.2016.00043.

[5] P. N. Gawande and S. S. Dambhare, "A novel algorithm to detect symmetrical faults during power swing for a double circuit multi-terminal transmission line," Proc. IEEE Power Eng. Soc. Transm. Distrib. Conf., vol. 2016-July, 2016, doi: 10.1109/TDC.2016.7519902.

[6] S. V. Unde and S. S. Dambhare, "Differential protection of mutually coupled lines in modal domain using synchronized measurements," 2016 Natl. Power Syst. Conf. NPSC 2016, 2017, doi: 10.1109/NPSC.2016.7858915.

[7] S. Unde, P. Gawande, and S. Dambhare, "New Algorithm for Protection of Double Circuit Transmission Lines Using Modal Currents," IEEE Trans. Power Deliv., vol. 34, no. 5, pp. 1967–1977, 2019, doi: 10.1109/TPWRD.2019.2906939.

[8] B. Bhalja and S. Purohit, "Protection of double-circuit transmission line using superimposed current," Electr. Power Components Syst., vol. 39, no. 6, pp. 590–604, 2011, doi: 10.1080/15325008.2010.528545.

[9] S. Li, W. Chen, Y. Tao, and D. Chen, "The simulation research of transverse differential protection based on impedance ratio for double circuit lines on the same tower," in 2015 5th International Conference on Electric Utility Deregulation and Restructuring and Power Technologies (DRPT), 2015, pp. 922–926.

[10] S. Anand, K. Kalita, and S. K. Parida, "Backup Protection for Mutually Coupled Double-Circuit Multisection Nonhomogeneous Transmission Lines Using Wide-Area Measurements," in 2021 IEEE 4th International Conference on Computing, Power and Communication Technologies (GUCON), 2021, pp. 1–6.

[11] S. K. Mishra, L. N. Tripathy, and S. C. Swain, "DWT approach based differential relaying scheme for single circuit and double circuit transmission line protection including STATCOM," Ain Shams Eng. J., vol. 10, no. 1, pp. 93–102, 2019, doi: 10.1016/j.asej.2018.02.002.

[12] D. Mourad, "Creative Cos-Sin Features for Double-Circuit Transmission Lines Protection Without Communication Channels," J. Control. Autom. Electr. Syst., vol. 32, no. 3, pp. 756–773, 2021, doi: 10.1007/s40313-021-00699-9.

[13] Y. Liu, Y. Zhu, and K. Wu, "CNN-Based Fault Phase Identification Method of Double Circuit Transmission Lines," Electr. Power Components Syst., vol. 48, no. 8, pp. 833–843, 2020, doi: 10.1080/15325008.2020.1821836.

[14] T. A. Kawady, G. M. Sowilam, and R. Shalwala, "Improved Distance Relaying for Double-Circuit Lines Using Adaptive Neuro-Fuzzy Inference System," Arab. J. Sci. Eng., vol. 45, no. 3, pp. 1969–1984, 2020, doi: 10.1007/s13369-020-04369-x.

[15] H. Seyedi, S. Teimourzadeh, and P. S. Nezhad, "Adaptive zero sequence compensation algorithm for double-circuit transmission line protection," IET Gener. Transm. Distrib., vol. 8, no. 6, pp. 1107–1116, 2014, doi: 10.1049/iet-gtd.2013.0538.

[16] A. Bachmatiuk and J. Izykowski, "Distance protection performance under inter-circuit faults on double-circuit transmission line," Prz. Elektrotechniczny, vol. 89, no. 1A, pp. 7–11, 2013.

[17] M. Forcan and Z. Stojanović, "A standby protection scheme to complement transverse differential protection of double circuit lines in the case of one parallel line tripped," Electr. Power Syst. Res., vol. 201, no. August, 2021, doi: 10.1016/j.epsr.2021.107570.

[18] N. Perera and A. D. Rajapakse, "Series-compensated double-circuit transmission-line protection using directions of current transients," IEEE Trans. Power Deliv., vol. 28, no. 3, pp. 1566–1575, 2013, doi: 10.1109/TPWRD.2013.2256934.

[19] G. Kapoor, N. Gautam, K. Jayaswal, and S. Tripathi, "Protection of Series Capacitor Compensated Double Circuit Transmission Line Using Wavelet Transform," 2019 IEEE 5th Int. Conf. Converg. Technol. I2CT 2019, pp. 1–8, 2019, doi: 10.1109/I2CT45611.2019.9033583.

[20] A. Swetapadma, P. Mishra, A. Yadav, and A. Y. Abdelaziz, "A non-unit protection scheme for double circuit series capacitor compensated transmission lines," Electr. Power Syst. Res., vol. 148, pp. 311–325,

2017, doi: 10.1016/j.epsr.2017.04.002.

[21] A. Swetapadma and A. Yadav, “An artificial neural network-based solution to locate the multilocation faults in double circuit series capacitor compensated transmission lines,” Int. Trans. Electr. Energy Syst., vol. 28, no. 4, pp. 1–20, 2018, doi: 10.1002/etep.2517.

[22] A. Yadav and A. Swetapadma, “Improved first zone reach setting of artificial neural network-based directional relay for protection of double circuit transmission lines,” IET Gener. Transm. Distrib., vol. 8, no. 3, pp. 373–388, 2014, doi: 10.1049/iet-gtd.2013.0239.

[23] N. Johannesson and S. Norrga, “Longitudinal differential protection based on the Universal Line Model,” IECON 2015 - 41st Annu. Conf. IEEE Ind. Electron. Soc., pp. 1091–1096, 2015, doi: 10.1109/IECON.2015.7392245.

[24] J. Izykowski and E. Rosolowski, “Application of synchronised distributed measurements to location of faults on overhead lines,” Prz. Elektrotechniczny, vol. 85, no. 11, pp. 21–25, 2009.

[25] A. Precise, “expansion planning, integer problems,” no. April, 2001.

[26] B. R. Bhalja and R. P. Maheshwari, “High-resistance faults on two terminal parallel transmission line: Analysis, simulation studies, and an adaptive distance relaying scheme,” IEEE Trans. Power Deliv., vol. 22, no. 2, pp. 801–812, 2007, doi: 10.1109/TPWRD.2007.893352.

[27] A. Halinka and M. Niedopytalski, “Evaluation of the correctness of operation of adaptive under-impedance criterion for HV single and double-circuit overhead power line with increased capacity,” Przegląd Elektrotechniczny, vol. 93, pp. 74–77, 2017.

[28] M. Kletsel and B. Mashrapov, “Traversal protection of two parallel lines without voltage path,” Prz. Elektrotechniczny, vol. 92, no. 2, pp. 168–170, 2016, doi: 10.15199/48.2016.02.45.

[29] M. K. (Mondal) and S. Debnath, “Fault location in UPFC compensated double circuit transmission line using negative sequence current phasors,” Electr. Power Syst. Res., vol. 184, no. February, p. 106347, 2020, doi: 10.1016/j.epsr.2020.106347.

[30] T. G. Bolandi, H. Seyedi, S. M. Hashemi, and P. S. Nezhad, “Impedance-Differential Protection: A New Approach to Transmission-Line Pilot Protection,” IEEE Trans. Power Deliv., vol. 30, no. 6, pp. 2510–2518, 2015, doi: 10.1109/TPWRD.2014.2387689.

[31] J. Herlender, K. Solak, and J. Iżykowski, “Impedance-differential protective algorithm for double-circuit transmission lines,” Prz. Elektrotechniczny, vol. 95, no. 11, pp. 240–244, 2019, doi: 10.15199/48.2019.11.55.